Chemosphere 213 (2018) 453–462

Contents lists available at ScienceDirect

Chemosphere

journal homepage: www.elsevier.com/locate/chemosphere

A molecular-scale study on the hydration of sulfuric acid-amide complexes and the atmospheric implication

Pu Ge [a], Gen Luo [a], Yi Luo [a, *], Wei Huang [b], Hongbin Xie [c], Jingwen Chen [c]

[a] State Key Laboratory of Fine Chemicals, School of Chemical Engineering, Dalian University of Technology, Dalian 116024, China
[b] School of Environmental Science & Optoelectronic Technology, University of Science and Technology of China, Hefei, Anhui 230026, China
[c] Key Laboratory of Industrial Ecology and Environmental Engineering (MOE), School of Environmental Science and Technology, Dalian University of Technology, Dalian 116024, China

HIGHLIGHTS

- No proton-transfer to C═O group occurs in formamide clusters.
- High concentration of formamide compensates its unfavorable interaction with SA.
- Proton transfer to water is significant when highly hydrated at low temperature.
- Interaction between SA and C═O group play important role in amide clusters.
- The amine substituent in amides affects the cluster structures and properties.

GRAPHICAL ABSTRACT

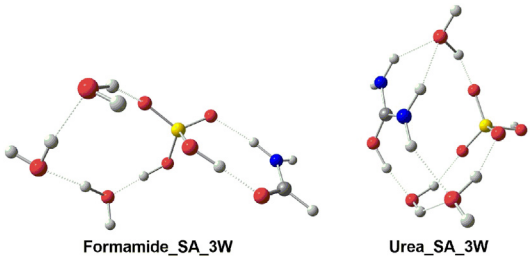

ARTICLE INFO

Article history:
Received 12 July 2018
Received in revised form
6 September 2018
Accepted 12 September 2018
Available online 15 September 2018

Handling Editor: R Ebinghaus

Keywords:
Urea
Formamide
GRRM
New particle formation
Amine group
Hydration

ABSTRACT

Amides are ubiquitous in atmosphere. However, the role of amides in new particle formation (NPF) is poorly understood. Herein, the interaction of urea and formamide with sulfuric acid (SA) and up to four water (W) molecules has been studied at the M06-2X/6-311++G(3df,3pd) level of theory. The structures and properties of (Formamide)(SA)$(W)_n$ (n = 0–4) and (Urea)(SA)$(W)_n$ (n = 0–4) clusters were investigated. Results show that the interaction of SA with the C═O group of amides plays a more important role in amide clusters compared with the NH_2 group. Proton transfer to water molecule become dominant in highly hydrated amide clusters at lower temperatures. There is no proton transfer to C═O group in formamide clusters. The Rayleigh light scattering intensities of amide clusters are comparable to that of amine and oxalic acid clusters reported previously. Moreover, unhydrated (Amide)(SA) clusters have similar or even higher ability than hydrated SA clusters to participate in ion-induced nucleation. In comparison with formamide, urea has more interacting sites and its clusters have higher Rayleigh light scattering intensities, larger dipole moment, stronger interaction with SA and lower water affinity. The intermolecular interaction in (Formamide)(SA) is slightly weaker than that of SA dimer, which may be compensated by the high concentration of formamide, thus enabling formamide to participate in initial steps of NPF. This study may bring new insight into the role of amides in initial steps of NPF from molecular scale and could help better understand the properties of amide-containing organic aerosol.

* Corresponding author.
E-mail address: luoyi@dlut.edu.cn (Y. Luo).

https://doi.org/10.1016/j.chemosphere.2018.09.068
0045-6535/

1. Introduction

Aerosols impact climate forcing (Haywood and Boucher, 2000), air quality (Von Schneidemesser et al., 2015) and public health (Dimitriou and Kassomenos, 2017; Saikia et al., 2016). Improving knowledge about the formation process of aerosol particles is necessary to evaluate their effects. A main origin of atmospheric aerosols is new particle formation (NPF) which comprises nucleation process and subsequent growth (Zhang et al., 2011). Sulfuric acid (SA) is a key component in nucleation (Kuang et al., 2008). Besides, the prominent enhancing effect of organics has been proposed (Almeida et al., 2013). Studies show that one SA molecule and one organic molecule could be involved in the rate-limiting step of the nucleation process (Xie et al., 2017a; Metzger et al., 2010). Olenius pointed out that the strong interaction of dimethylamine (DMA) and SA could lead to a barrierless nucleation process by addition of (DMA)(SA) cluster (Olenius et al., 2013). The enhancing ability of organics in NPF could be evaluated by their interaction with SA.

Among the 160 different organic NH_x-containing compounds identified in the atmosphere (Ge et al., 2011), there are about 80 species for which the molecules contain substructures of NH_x ($x = 1, 2$) connecting to π bonds, featuring a p-π conjugate structure (Xie et al., 2017b). Amides could be the most abundant in these p-π conjugate compounds which could reach the few ppbv level in urban Shanghai, China (Yao et al., 2016). The detection of high concentrations of amides in the ambient air urges a complete understanding on their atmospheric sinks. Formamide, as the simplest amide, is a high production volume chemical with an annual global production of several hundred thousand tons (Bunkan et al., 2016). Extensive studies focus on the atmospheric origin of formamide as the major oxidation product of monoethanolamine (MEA) (Xie et al., 2014; Zhu et al., 2013) and methylamine (MA) (Borduas et al., 2016). Besides, the oxidation of formamide has been widely studied to form isocyanic acid (Bunkan et al., 2016; Borduas et al., 2015). Formamide has also been detected in atmospheric particles (Ge et al., 2011). Therefore there is a possible removal of formamide by interaction with SA due to participation in NPF as a sink for formamide. The enhancing ability of amides to NPF has been studied by many researchers. Glasoe pointed out that urea and acetamide have enhancing effect toward nucleation but are much weaker than amines (Glasoe et al., 2015). Recently, Kumar demonstrated that urea could stabilizing SA by forming the strongest clusters compared with nitric acid, methanesulfuric acid and formic acid, thus may play an important role in NPF (Kumar et al., 2018). Besides, Chen suggested that gaseous alkylamides could be uptaken by suspended SA particles and measured their multiphase uptake coefficients (Chen et al., 2017a). However, the role of formamide as potential nucleation stabilizer remains almost unexplored.

In spite of the pioneering work by Kumar, knowledge on the detailed information of proton transfer and the properties of urea clusters is limited. Amine group in urea clusters is not the proton acceptor as in the case of alkylamine (Kumar et al., 2018). The effects of amine group, acting as substituent, on the cluster structures and properties together with the effect on the stabilizing ability of urea towards SA are unexplored, which may enrich the chemistry of amine functional group in NPF. Formamide and urea, differing by an amine substitution, may have different performance on the initial steps of NPF. Besides, by investigating urea and formamide clusters, some distinct characteristics of amide clusters could be elucidated, therefore providing a more comprehensive knowledge on the role of amides in NPF.

In this study, the interaction of formamide and urea with SA has been computationally studied to evaluate the enhancing ability of amides in initial steps of NPF, the characteristics of amide clusters and the effects of amine substitution. In view of that hydration could affect nucleation rates by affecting the mobility, stability and lifetime of clusters (Nadykto et al., 2009) and could promote proton transfer in clusters (Temelso et al., 2012a; Miao et al., 2015), hydration effect was therefore also considered with up to four water (W) molecules (Kumar et al., 2018) to investigate the proton transfer in amide clusters. The structures and properties of (Urea)(SA)$(W)_n$ and (Formamide)(SA)$(W)_n$ ($n = 0–4$) clusters were presented. Besides, the effects of amine substitution were also discussed.

2. Computational details

In this study, the Global Reaction Route Mapping (GRRM) program (version 14) was used in combination with the Gaussian 09 program package (Frisch et al., 2009) to search for the global minima of (Urea)(SA)$(W)_n$ and (Formamide)(SA)$(W)_n$ ($n = 0–4$) clusters. The scaled hypersphere search (SHS) method, which is an uphill-walking technique, was utilized to automatically explore the reaction pathway from a given equilibrium structure (EQ) (Maeda and Ohno, 2005; Ohno and Maeda, 2004, 2006). Such an exploration of reaction pathways is executed by detecting and following anharmonic downward distortions (ADDs) (Maeda and Ohno, 2008). This ADD following is a new concept based on a kind of principle that has arisen from deep considerations on the feature of potential energy surface (PES). To effectively detect the ADD, a given EQ-centered hypersphere surface is introduced in the SHS technique. During the reaction pathway following on the scaled hypersphere surface, the conventional optimization scheme and downhill-walking technique may be utilized. By detecting and following all of the ADDs for a given EQ, the SHS method can find transition states, dissociation channels, and other EQs. Such detection and following are automatically done for each newly found EQ via a one-after-another manner. Since the occurrence of a chemical reaction shows an ADD as a symptom and the lowest-energy minimum should not be out of connection with other EQs on the global PES, most of the important EQs at the low-energy region should be found by the SHS method. After the reaction pathways are traced for all the obtained EQs, the global potential energy surface may be figured. As shown in the applications to $(H_2O)_8$ and $H^+(H_2O)_8$, the search for known important structures as well as global potential energy minimum of H-bond clusters has been achieved (Maeda and Ohno, 2007; Luo et al., 2007). Specifically, molecular energy and its gradient (Hessian matrix) were calculated at the HF/6-31G level for efficiency of exploration (Lin et al., 2014). The following conditions were imposed on GRRM calculations: (1) start with 24 randomly created conformations; (2) to accelerate pathway exploration via ADD, the largest ADD (LADD) technique was applied by setting the parameter LADD to be 5; (3) optimize the structure only for EQs and skip the optimization of the transition structures (Omori et al., 2014).

Since over 1000 isomers were obtained for larger clusters, isomers within a certain energy range were selected for optimization. As the cluster systems become larger and the configurations get more complex, the energy difference between the isomers gets smaller due to the flexible hydrogen bond networks, thus an energy range of 4–7 kcal/mol of the global minimum is identified for different sizes of (Urea)(SA)$(W)_n$ and (Formamide)(SA)$(W)_n$ ($n = 0–4$) clusters. The obtained geometries were re-optimized at the level of M06-2X/6-311++G(3df,3pd) (Zhao and Truhlar, 2007). Frequency calculations were operated for each stationary point to identify the structure is a stable one. Such a method was reported to give reasonable results for similar clusters (Elm et al., 2012; Ge et al., 2018). In order to evaluate the reliability of the M06-2X

functional in the current system, the formation Gibbs free energies of clusters (Formamide)(SA) and (SA)(W) have been calculated by using B3LYP, B3PW91, CAM-B3LYP, M06-2X, PW91PW91, and ωB97X-D methods together with 6−311++G(3df,3pd) basis set. The results of all the functionals were compared with those of Møller-Plesset perturbation theory (MP2) to investigate their performances. The results of the benchmark are shown in Table S1 in Supporting Information (SI). The mean unsigned deviation (MUD) in Table S1 indicates that CAM-B3LYP, M06-2X and PW91PW91 with 6−311++G(3df,3pd) basis set match the MP2 results, with MUD between 0.11 and 0.34 kcal/mol for the test clusters. Besides, the deviation of the formation Gibbs free energies for (Formamide)(SA) is smallest by M06-2X method with value of 0.11 kcal/mol. Thus M06-2X method was chosen to obtain the structures and energies in this study. In addition, M06-2X method is adopted in the previous study of urea clusters by Kumar (Kumar et al., 2018), which further indicates its validity towards amide clusters. The variations of Rayleigh light scattering intensities, R_n, along with the number of water molecules were calculated at the CAM-B3LYP/aug-cc-pVDZ level of theory, which has been demonstrated to have a good balance between efficiency and accuracy (Elm et al., 2014a; Peng et al., 2015a). The specific formulas for such calculations have been given elsewhere (Elm et al., 2014a).

3. Results and discussion

3.1. Structures

In this study, we use **Amide_SA_*m*W_*n*** notation to present the conformations of (Urea)(SA)$(W)_n$ and (Formamide)(SA)$(W)_n$ (n = 0−4) clusters. Here, "*m*" denotes the number of water molecules, "*n*" is used to differentiate various isomers of one cluster, arranged in order of increasing relative electronic energy. All the isomers along with the relative electronic energies (Δ*E*) and relative Gibbs free energies (Δ*G*) are presented in Figs. S1−S10. The lowest electronic energy and lowest Gibbs free energy isomers of each (Urea)(SA)$(W)_n$ and (Formamide)(SA)$(W)_n$ (n = 0−4) cluster are presented in Fig. 1. For a clearer illustration, the lowest Gibbs free energy structures and lowest electronic energy structures are further demonstrated as **Amide_SA_*m*W_G** and **Amide_SA_*m*W_E**, respectively, while **Amide_SA_*m*W_EG** represents structures being both the lowest Gibbs free energy and electronic energy one. As shown in Fig. 1a and b, in **Formamide_SA_EG**, SA interacts with both NH_2 and C═O groups of formamide, forming a cyclic structure. The structure of **Urea_SA_EG** is similar, which is consistent with previous study (Kumar et al., 2018), indicating that amides tend to form cyclic structure with SA. The lowest Gibbs free energy structures of amide clusters are similar upon addition of up to two water molecules. The intermolecular hydrogen bond H···O between C═O group (acceptor) and SA is shorter than that between NH_2 group (donor) and SA (1.5 *vs*. 1.9 Å). Meanwhile, the electron densities of hydrogen bond C═O···H of **Formamide_SA_EG** and **Urea_SA_EG** are 0.0798 and 0.0925 a.u., respectively, larger than that (0.0277 and 0.0283 a.u.) for S═O···H hydrogen bond (Fig. S11). These results indicate that C═O group may play more important role in the interaction of amides with SA, which can also be demonstrated by the fact that **Formamide_SA_c** with C═O interacting with SA is about 8 kcal/mol more stable than **Formamide_SA_d**, as listed in Fig. 1c. The lowest Gibbs free energy structures of amide clusters become different with three water molecules. The structure of **Urea_SA_3W_EG** transforms from linear to spherical while **Formamide_SA_3W_G** remains linear structure with a larger hydrated sulfuric acid ring. With four water molecules, amide clusters all transform to spherical structures. As for the lowest electronic energy structures, the two amide clusters with two water molecules become structurally different, as indicated by **Urea_SA_2W_E and Formamide_SA_2W_EG**. The differences of cluster structures may be partly due to the presence of additional amine group in urea providing more interaction sites, as indicated by four hydrogen bonds in **Urea_SA_3W_EG** and three in **Urea_SA_4W_G** compared with two hydrogen bonds in **Formamide_SA_3W_G** and **Formamide_SA_4W_EG**.

Proton transfer occurs in hydrated amide clusters. However, proton transfer is different between urea and formamide clusters. A proton of SA transfers only to water molecule in formamide clusters while to C═O group or water molecule in urea clusters (Figs. S1−10). More specifically, first proton transfer occurs when two water molecules are added in two isomers **Formamide_SA_2W_b** and **Formamide_SA_2W_h**, as indicated in Fig. 1c. Proton transfer become important in formamide clusters with three water molecules, and nearly all the isomers of (Formamide)(SA)$(W)_3$ undergo proton transfer, including **Formamide_SA_3W_E** (Fig. 1a). All the isomers of (Formamide)(SA)$(W)_4$ exhibit proton transfer from SA to water molecule. The case is quite different in urea clusters. Proton transfer occurs earlier in urea clusters upon addition of first water molecule in two isomers **Urea_SA_1W_d** and **Urea_SA_1W_g**, as is shown in Fig. 1c. **Urea_SA_1W_d** with proton transfer to C═O group is more stable than **Urea_SA_1W_g** with proton transfer to water molecule. In (Urea)(SA)$(W)_2$, most of the isomers undergo proton transfer. The isomers with proton transfer to urea are more than to water. In **Urea_SA_2W_E** (Fig. 1b), proton transfers to urea molecule, which is consistent with Kumar's work (Kumar et al., 2018). The relative importance of the two kinds of proton transfer starts to change with three water molecules. Proton transfer occurs in all the isomers of (Urea)(SA)$(W)_3$. The isomers with proton transfer to water molecule are more than that to urea, although the proton transfer to urea occurs in **Urea_SA_3W_EG**, the lowest isomer in both free energy and electronic energy. In (Urea)(SA)$(W)_4$, the proportion of proton transfer to water molecule further increases and exceeds that of (Urea)(SA)$(W)_3$. Proton transfer to water molecule occurs in **Urea_SA_4W_E** (Fig. 1b). The results demonstrate that proton transfer in amide clusters is various with different amide compounds. Moreover, when in highly hydrated conditions, proton transfer to water become important in amide clusters. These results may imply that the existing form of amides and their effect on properties of aerosols may depend on the specific amide structures and the hydration conditions.

3.2. Temperature dependence of amide clusters

Previous studies have revealed that the thermodynamic properties and the stability order of isomers may change at different temperatures (Ge et al., 2018), which would drop along with increase in altitude. Thus, understanding the temperature dependence of amide clusters is important for elucidating the relative importance of various structure types under specific conditions. The population distributions of the isomers for (Formamide)(SA)$(W)_n$ (n = 0−4) and (Urea)(SA)$(W)_n$ (n = 0−4) clusters *versus* the temperature, ranging from 150 to 300 K, are presented in Fig. 2 and Fig. S12. The methods used are presented elsewhere (Chen et al., 2017b).

The proportion of **Formamide_SA_EG**, **Formamide_SA_1W_EG** and **Formamide_SA_2W_EG** clusters remains almost constant with a share of practically 100 percent in the temperature range of 150−300 K (Fig. S12). This suggests that the contribution from the global minimum, which is the most common conformer in the population, is important for the ensemble of energetically accessible conformations in formamide clusters (Partanen et al., 2016). Furthermore, this indicates that there is no proton transfer in less

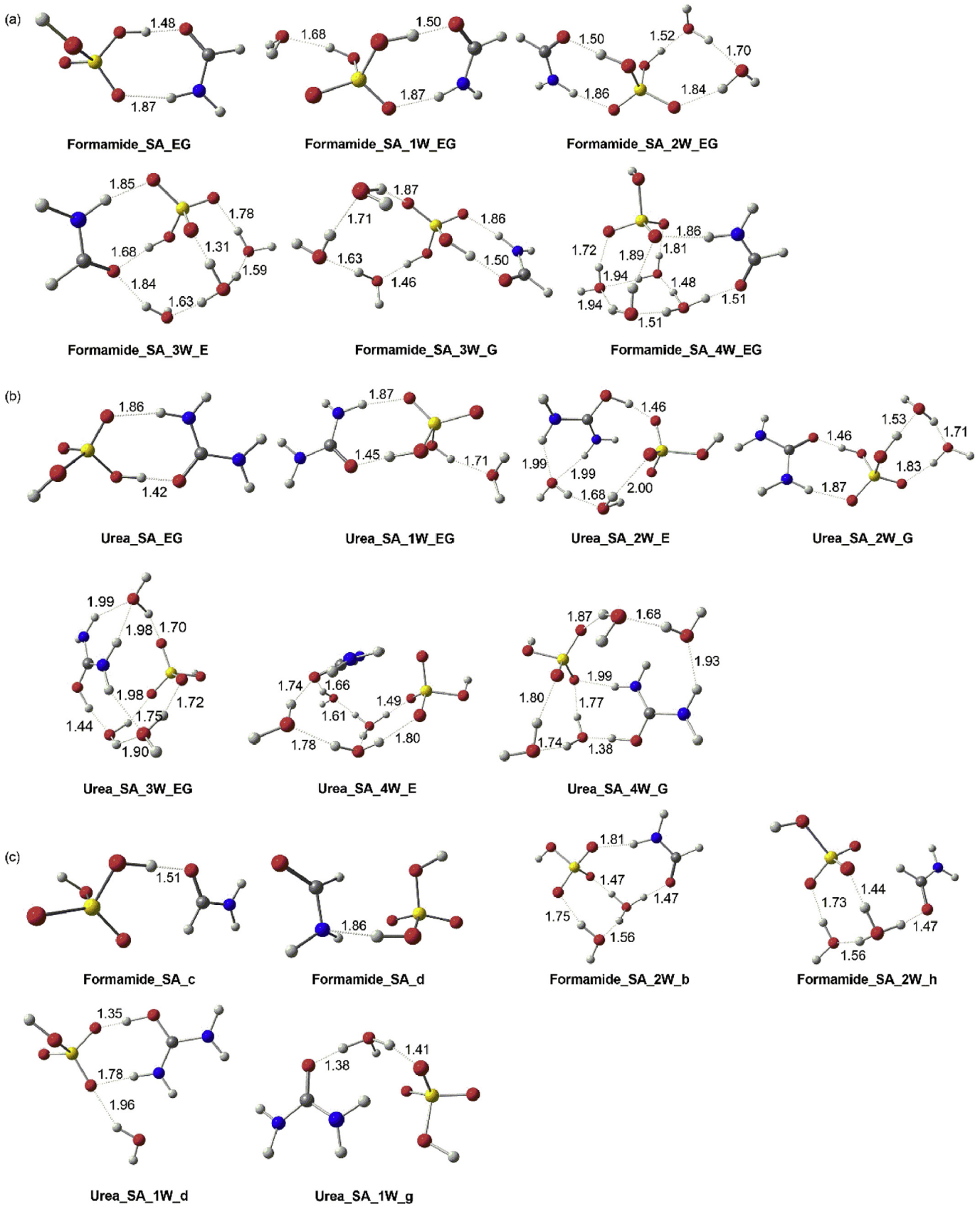

Fig. 1. The selected structures of (Urea)(SA)$(W)_n$ and (Formamide)(SA)$(W)_n$ (n = 0–4) at the M06-2X/6-311++G(3df,3pd) level of theory (oxygen in red, hydrogen in white, sulfur in yellow, carbon in gray and nitrogen in blue). The hydrogen bond lengths are given in Å. (For interpretation of the references to colour in this figure legend, the reader is referred to the Web version of this article.)

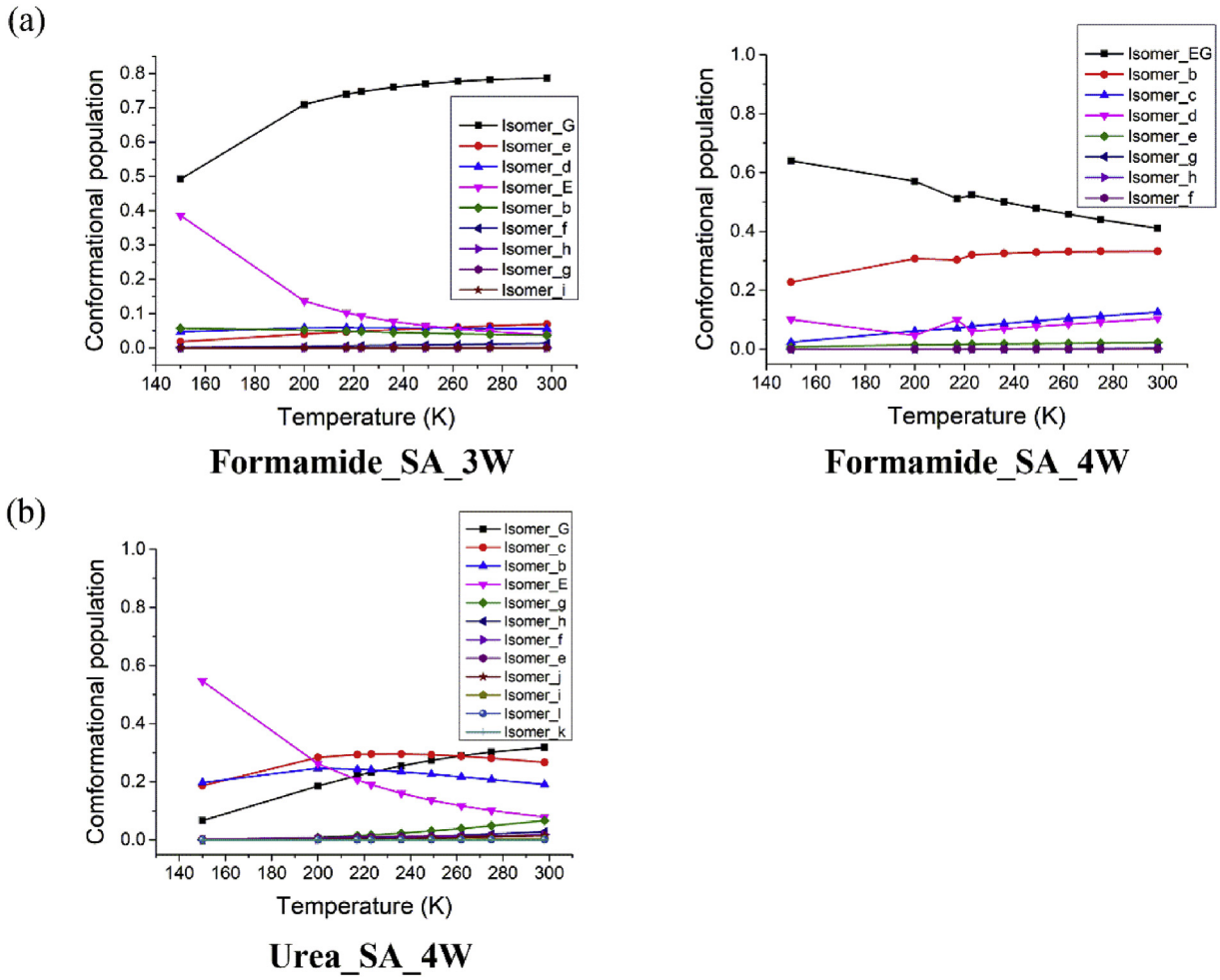

Fig. 2. The conformational population changes with the temperature for (a) (Formamide)(SA)$(W)_n$ (n = 3, 4) and (b) (Urea)(SA)$(W)_4$ clusters.

hydrated formamide clusters. The isomer populations of (Formamide)(SA)$(W)_3$ and (Formamide)(SA)$(W)_4$ change significantly with temperature, as shown in Fig. 2a. The **Formamide_SA_3W_G** is most common at 300 K, but its population drops significantly from 80% to 50% as temperature decreases from 300 to 150 K. The proportion of **Formamide_SA_3W_E** increases from 7% to 40%. This indicates that proton transfer to water molecules gradually becomes dominant in formamide clusters in low temperature with addition of three water molecules. **Formamide_SA_4W_EG** and **Formamide_SA_4W_b** are comparable at 300 K. As the temperature decreases, the population of **Formamide_SA_4W_EG** increases to 65% while **Formamide_SA_4W_b** decreases to 20%. For urea clusters, the calculated population (Fig. S12) suggests that **Urea_SA_EG**, **Urea_SA_1W_EG**, **Urea_SA_2W_G** and **Urea_SA_3W_EG** play a dominant role at the considered temperature range. The other isomers are negligible for these clusters. This indicates that there is no proton transfer in low hydrated urea clusters. However, with addition of three water molecules, cluster with proton transfer to urea has the greatest weight in the ensemble of conformers at all temperatures. The variations of isomers of (Urea)(SA)$(W)_4$ are diverse according to Fig. 2. The proportions of **Urea_SA_4W_E**, **Urea_SA_4W_b**, **Urea_SA_4W_c** and **Urea_SA_4W_G** are comparable in 300 K while **Urea_SA_4W_E** increases and **Urea_SA_4W_G** decreases with **Urea_SA_4W_b** and **Urea_SA_4W_c** remaining almost constant when temperature drops. When temperature is below 200 K, the proportion of **Urea_SA_4W_E** increases rapidly, which becomes the most prevalent isomer. In **Urea_SA_4W_b**, **Urea_SA_4W_c** and **Urea_SA_4W_G**, proton transfers to urea molecule while in **Urea_SA_4W_E** to water molecules. This indicates that in highly hydrated urea clusters, isomers with proton transfer to urea molecule are prevalent when temperature is above 200 K while isomers with proton transfer to water molecule would become dominant in the temperatures below 200 K. To sum up, proton transfer in amide clusters only occurs in highly hydrated clusters with in formamide cluster to water molecule and in urea cluster to C═O group. Proton transfer to water molecule in highly hydrated urea clusters become dominant only at low temperature.

3.3. Thermodynamics

To investigate the thermodynamic stability of amide clusters, four different pathways of generating the (Amide)(SA)$(W)_n$ (n = 0–4) clusters were studied. In Stepwise binding path (**Stepwise_1W**), the affinity of water to amide-SA clusters is evaluated by ΔG(**Stepwise_1W**) = G(Amide)(SA)$(W)_n$ − G(Amide)(SA)$(W)_{n-1}$ − G(W). In Total binding path (**Total**), the stability of the clusters is evaluated by ΔG(**Total**) = G(Amide)(SA)$(W)_n$ − $n \times G$(W) − G(SA) − G(Amide). In Synthetic binding path of amide to (SA)$(W)_n$ (**Synthetic_Amide**), the affinity of amides to hydrated SA clusters is calculated as ΔG(**Synthetic_Amide**) = G(Amide)(SA)$(W)_n$ − G(SA)$(W)_n$ − G(Urea). In Synthetic binding path of sulfuric acid to (Amide)$(W)_n$ (**Synthetic_SA**), the interaction between SA and the

hydrated amide clusters is calculated as ΔG(**Synthetic_SA**) = G(Amide)(SA)$(W)_n$ − G(Amide)$(W)_n$ − G(SA). The corresponding formation Gibbs free energies (ΔG) associated with the four binding paths are displayed in Table 1. The formation electronic energies (ΔE) and formation enthalpies (ΔH) are listed in Tables S2 and S3. The structures of (SA)(SA) and (SA)$(W)_n$ (n = 1–4) clusters are listed in Figs. S13 and S14, which are consistent with previous works (Temelso et al., 2012a, 2012b). The structures of (Formamide)$(W)_n$ (n = 1–4) and (Urea)$(W)_n$ (n = 1–4) clusters are listed in Figs. S15 and S16.

The ΔG values of (SA)(W) and (SA)(SA) clusters calculated in this work are −2.51 and −8.41 kcal/mol, which are consistent with previous studies (Hanson and Eisele, 2000; Elm et al., 2014b). As can be seen from Table 1, the formation of (Urea)(SA) clusters is more favorable than that of (SA)(W) and (SA)(SA) clusters, with ΔG values of −10.86 kcal/mol. This indicates that urea is capable of forming stable pre-nucleation clusters with SA, which is consistent with Kumar's work (Kumar et al., 2018). The formation Gibbs free energy of (Formamide)(SA) is only −8.01 kcal/mol, lower than that of (SA)(SA) and (Urea)(SA) clusters. The energies corrected by Basis Set Superposition Error (BSSE) listed in Table S4 are also consistent with the above results. As formamide and urea differ by an amine substituent in structure, this result reveals the significant effect of amine group towards amides on stabilizing SA. Besides, the interaction of (Formamide)(SA) (−8.01 kcal/mol without BSSE and −7.21 kcal/mol with BSSE) is comparable to that of $(NH_3)(H_2SO_4)$ (−7.84 kcal/mol without BSSE and −7.28 kcal/mol with BSSE) calculated at the same level M06-2X/6-311++G(3df,3pd) reported previously (Elm et al., 2012).

In **Total** path, the interaction energies become more negative with the increase of water molecules, which suggests the stability of water-enriched amide clusters. In **Synthetic_Amide** path, the affinity of urea and formamide to hydrated SA clusters is gradually weakened as the water content grows. This may suggest that the effect of amides decreases with the water saturation ratio increases, which is similar to the case of ammonia (Nadykto and Yu, 2007). In **Synthetic_Amide** path, the binding free energies of hydrated urea clusters are disfavored by 0.69–4.37 kcal/mol (0.69 kcal/mol in (Urea)(SA)(W), 2.01 kcal/mol in (Urea)(SA)$(W)_2$, 2.40 kcal/mol in (Urea)(SA)$(W)_3$ and 4.37 kcal/mol in (Urea)(SA)$(W)_4$) compared with (Urea)(SA) while the electronic energies are enhanced by 8–12 kcal/mol (Fig. S1), which is consistent with previous study (Kumar et al., 2018). In **Synthetic_SA** path, the interaction between SA and the hydrated amide clusters becomes stronger with more water molecules, possibly due to the strong interaction between SA and water molecules because of the high hygroscopicity of SA. Combining **Synthetic_SA** path and **Synthetic_Amide** path, one could conclude that the interaction between SA and hydrated amides is strongly dependent on the degree of hydration of amides. The hydration of SA decreases while the hydration of amides increases the interaction between amides and SA. According to **Stepwise_1W** path, the interaction in formamide and urea clusters is weaker than that of corresponding hydrated SA, which are −2.51, −2.52, −1.81, and −1.73 kcal/mol for (SA)(W), (SA)$(W)_2$, (SA)$(W)_3$, and (SA)$(W)_4$, respectively. This indicates that the presence of amides is unlikely to enhance the affinity of water to hydrated SA clusters.

3.4. Hydrate distribution and influence of humidity

Hydration affects proton transfer in (Urea)(SA)$(W)_n$ (n = 0–4) and (Formamide)(SA)$(W)_n$ (n = 0–4) clusters. However, the number of water molecules in the clusters is affected by the relative humidity (RH). To assess the extent of hydration under different circumstances, we calculated the hydrate distributions for amide clusters by using the method reported previously (Noppel et al., 2002). Fig. 3 indicates the calculated hydrate distributions of (Urea)(SA)$(W)_n$ (n = 0–4) and (Formamide)(SA)$(W)_n$ (n = 0–4) clusters at five different relative humidity values (20%, 40%, 60%, 80%, 100%) at 298.15 K.

As shown in Fig. 3a, the total concentration of the (Formamide)(SA)$(W)_n$ (n = 0–4) clusters is mainly dispersed as un-, mono- and dihydrates. When RH is close to 40%, about 50% of the clusters are hydrated. As RH increases from 20% to 60%, the most prevalent specie changes from unhydrated clusters to monohydrated clusters. When RH is above 60%, the percentage of unhydrated clusters decreases and dihydrates increases to about 30% at 80% RH while monohydrates remains almost constant. The hydration distributions for (Urea)(SA)$(W)_n$ (n = 0–4) clusters are different. The unhydrates dominate the cluster distribution at all RH. With increasing RH, the percentage of unhydrated clusters gradually decreases from about 90% to 50%, while the percentage of monohydrates, dihydrates and trihydrates increases gradually from 10% to 40%, 0.5%–10% and 0.1%–5%, respectively. Larger hydrates are almost nonexistent at all RH for both formamide and urea clusters. As shown in Fig. 3, the dominant clusters are unhydrates in urea clusters all the time while shift from unhydrates to monohydrates in formamide clusters, indicating that the ability of formamide clusters to retain water molecule is stronger than urea clusters, which is consistent with the relatively stronger interaction of formamide clusters with water in **Stepwise_1W** path (Table 1) upon addition of up to two water molecules. Moreover, this suggests that amine group in amides may decrease the water affinity of amide clusters.

3.5. Optical properties

The Rayleigh light scattering is the dominant mechanism of the

Table 1
The Gibbs free energies associated with the formation of (Urea)(SA)$(W)_n$ (n = 0–4) and (Formamide)(SA)$(W)_n$ (n = 0–4) clusters through four paths. Energies are in kcal/mol.

Isomer	Stepwise_1W	Total	Synthetic_Amide	Synthetic_SA
(Urea)(SA)$(W)_n$ (n = 0–4) clusters				
(Urea)(SA)		−10.86	−10.86	−10.86
(Urea)(SA)$(W)_1$	−1.83	−12.69	−10.17	−13.16
(Urea)(SA)$(W)_2$	−1.19	−13.88	−8.85	−14.12
(Urea)(SA)$(W)_3$	−1.42	−15.30	−8.46	−16.41
(Urea)(SA)$(W)_4$	0.24	−15.06	−6.49	−16.27
(Formamide)(SA)$(W)_n$ (n = 0–4) clusters				
(Formamide)(SA)		−8.01	−8.01	−8.01
(Formamide)(SA)$(W)_1$	−2.39	−10.40	−7.89	−11.22
(Formamide)(SA)$(W)_2$	−1.87	−12.27	−7.24	−13.82
(Formamide)(SA)$(W)_3$	0.89	−11.38	−4.53	−14.53
(Formamide)(SA)$(W)_4$	−0.41	−11.78	−3.21	−16.25

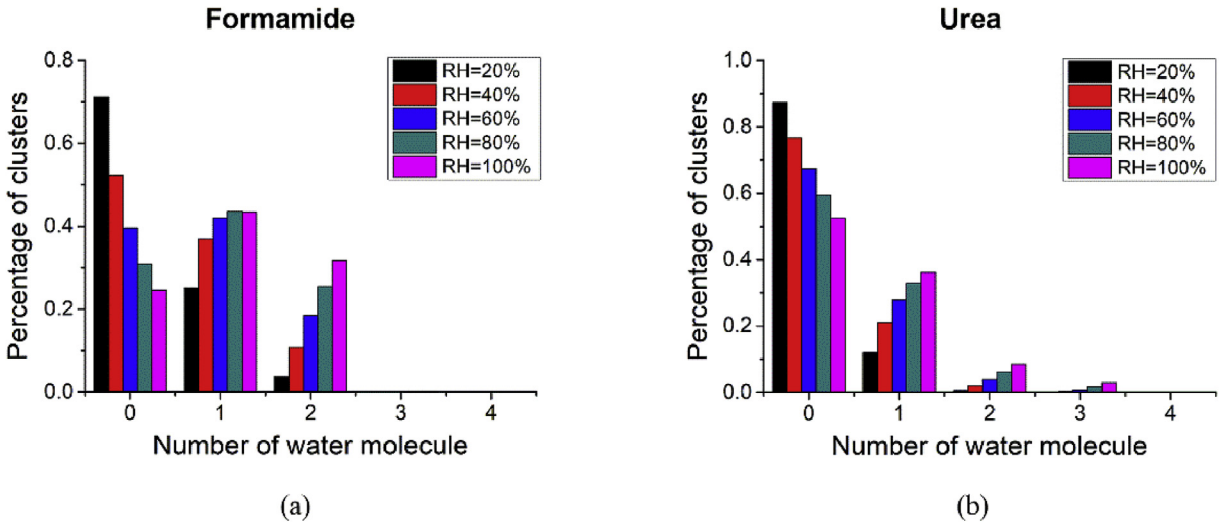

Fig. 3. Hydrate distributions of (a) (Formamide)(SA)$(W)_n$ (n = 0–4) and (b) (Urea)(SA)$(W)_n$ (n = 0–4) clusters at five different relative humidities at 298.15 K.

extinction properties of pre-nucleation clusters which could directly reduce atmospheric visibility. Therefore the Rayleigh light scattering intensities were investigated for amide clusters. The variations of Rayleigh light scattering intensities along with number of water molecules for (Formamide)(SA)$(W)_n$ (n = 0–4) and (Urea)(SA)$(W)_n$ (n = 0–4) clusters are displayed in Fig. 4. The Rayleigh light intensity increases along with the number of water molecules, which is consistent with previous study (Elm et al., 2014a). The Rayleigh light intensities range from 2.6×10^5–5.8×10^5 a.u. for (Urea)(SA)$(W)_n$ (n = 0–4) and 2.0×10^5–4.9×10^5 a.u. for (Formamide)(SA)$(W)_n$ (n = 0–4), which are comparable to that of $(H_2C_2O_4)(NH_3)_2(H_2O)_n$ (n = 0–3) (Peng et al., 2016), $(H_2C_2O_4)(NH_3)_n$ (n = 0–5) (Peng et al., 2015b), $(H_2C_2O_4)(H_2SO_4)(W)_n$ (n = 0–4) (Miao et al., 2015) and $(CH_3NH_2)(H_2SO_4)_2(W)_n$ (n = 0–2) (Lv et al., 2015) clusters reported previously. Besides, the Rayleigh light intensities of (Urea)(SA)$(W)_n$ (n = 0–4) are greater by nearly 5.0×10^4–9.0×10^4 a.u. than (Formamide)(SA)$(W)_n$ (n = 0–4), which indicates the enhancing effect of amine substituent.

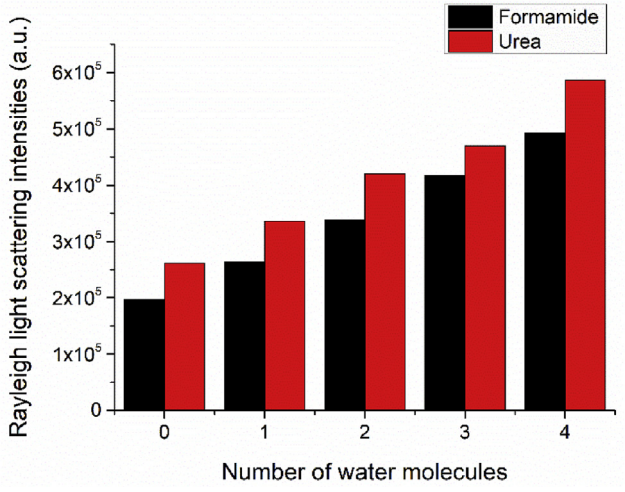

Fig. 4. Rayleigh light scattering intensities of (Formamide)(SA)$(W)_n$ (n = 0–4) and (Urea)(SA)$(W)_n$ (n = 0–4) clusters as a function of the number of water molecules.

3.6. Atmospheric implication

The formation of new particles has previously been shown to be very dependent on the formation of SA dimers as a starting point for further growth (Olenius et al., 2013; Elm et al., 2016). Thus the comparison of the interaction of the heterodimer with SA dimer is important to evaluate the nucleation ability of the organics. To estimate the atmospheric impact of amides, we compared reaction R1 and R2 with reaction R3.

$$H_2SO_4 + H_2SO_4 \rightleftharpoons (H_2SO_4)(H_2SO_4) \quad (R1)$$

$$NH_2CHO + H_2SO_4 \rightleftharpoons (NH_2SO_4)(H_2SO_4) \quad (R2)$$

$$(NH_2)_2CO + H_2SO_4 \rightleftharpoons [(NH_2)_2CO)](H_2SO_4) \quad (R3)$$

Assuming mass-balance relations, the following equilibrium conditions were set up:

$$K_1 = \frac{[(H_2SO_4)_2]}{[H_2SO_4]^2} = \exp\left(-\frac{\Delta G_1}{RT}\right) \quad (1)$$

$$K_2 = \frac{[(NH_2CHO)(H_2SO_4)]}{[NH_2CHO][H_2SO_4]} = \exp\left(-\frac{\Delta G_2}{RT}\right) \quad (2)$$

$$K_3 = \frac{[((NH_2)_2CO)(H_2SO_4)]}{[((NH_2)_2CO)][H_2SO_4]} = \exp\left(-\frac{\Delta G_3}{RT}\right) \quad (3)$$

To estimate at which point amide compounds become equally as important as SA, we found the ratio between the concentrations $[(H_2SO_4)_2]$ and $[(NH_2CHO)(H_2SO_4)]$, $[(H_2SO_4)_2]$ and $[((NH_2)_2CHO)(H_2SO_4)]$ and divided K_1 with K_2, K_1 with K_3:

$$\frac{K_1}{K_2} = \frac{[NH_2CHO]}{[H_2SO_4]} = \exp\left(\frac{\Delta G_2 - \Delta G_1}{RT}\right) \quad (4)$$

$$\frac{K_1}{K_3} = \frac{[(NH_2)_2CO]}{[H_2SO_4]} = \exp\left(\frac{\Delta G_3 - \Delta G_1}{RT}\right) \quad (5)$$

From Table 1, this corresponds to a (ΔG_2 - ΔG_1) value of 0.4 kcal/mol and (ΔG_3 - ΔG_1) value of −2.45 kcal/mol. Thus K_1/K_2 value of 2 and K_1/K_3 value of 10^{-2} were obtained accordingly. Atmospheric

concentrations of SA are typically found in the range of 10^6-10^7 molecules/cm^3 (Zhao et al., 2017). This implies that concentrations of urea approximately 10^2 lower than SA (i.e. as low as 10^4-10^5 molecules/cm^3) while formamide about two times higher than SA (i.e. 10^6-10^7 molecule/cm^3) will yield the same stability for forming the dimer cluster, therefore playing an important role in stabilizing SA to NPF. Formamide is the major oxidation product of monoethanolamine (MEA) (Nielsen et al., 2011), which could reach up to 10 ppbv (Borduas et al., 2016), due to the large-scale emission of MEA from post-combustion CO_2 capture facility (Zhu et al., 2013). Besides, formamide is also the oxidation product of methylamine which exists in certain concentration ranging from 1.9 pptv to 0.12 ppmv in atmosphere (Ge et al., 2011), with yield in OH-initiated degradation of MA and DMA in the presence of NO_x about 11% (Nielsen et al., 2012). In this case, the concentration of formamide in atmosphere may be times of SA concentration, thus enabling formamide to participate in initial steps of NPF.

It should also be noted that only thermodynamic cluster stabilities were considered while kinetic limitations would also inevitably restrict the atmospheric role of amides. The cluster evaporation rates based on the formation free energy gained by quantum chemical calculation have been identified to be a critical kinetic parameter to investigate the very early stages of particle formation (Ortega et al., 2012). Evaporation rates of urea and formamide of (Urea)(SA)$(W)_n$ (n = 0–4) and (Formamide)(SA)$(W)_n$ (n = 0–4) clusters were investigated. The evaporation rates of formamide in (Formamide)(SA) cluster are about 10^2 times higher than that of urea in (Urea)(SA) (Table S5). This indicates that the concentration of formamide may need to be over 10^2 times higher than that of urea to compete with urea. This is consistent with the concentration level obtained above by thermodynamic analysis. Meanwhile, the evaporation rates of amides become larger with increasing number of water molecules. This means that in hydrated clusters, a higher concentration of amides is needed in order to reach a high enough collision probability to participate in NPF.

3.7. The participation of (Amide)(SA) in ion-induced nucleation

Nadykto pointed out that the electrical dipole moment of stable hydrogen-bonded clusters of sulfuric acid is important for ion-induced nucleation, which is largely controlled by dipole-charge interaction of airborne ions with vapor monomers and pre-existing clusters (Nadykto, 2003). The immediate vicinity (<1 kcal/mol) of the global minima may be populated with a number of isomers with drastically different dipole moment, leading to strong dipole-ion interaction strength (Nadykto and Yu, 2008). The dipole moment of all the isomers of (Formamide)(SA)$(W)_n$ (n = 0–4) and (Urea)(SA)$(W)_n$ (n = 0–4) clusters is listed in Table S6. The highest dipole moment was identified among isomers within 1 kcal/mol of the global Gibbs free energy minimum for each cluster of (Formamide)(SA)$(W)_n$ (n = 0–4) and (Urea)(SA)$(W)_n$ (n = 0–4). The structures of the corresponding isomers and their dipole moment are listed in Fig. 5. As shown in Fig. 5a, unhydrated **Urea_SA_EG** and **Formamide_SA_EG** possess higher dipole moment (5.06 and 6.57 Debye) than their corresponding hydrated clusters, indicating that hydration may weaken the ion-dipole interaction of amide clusters, which needs further validation by experiments. Although there is an increase in dipole

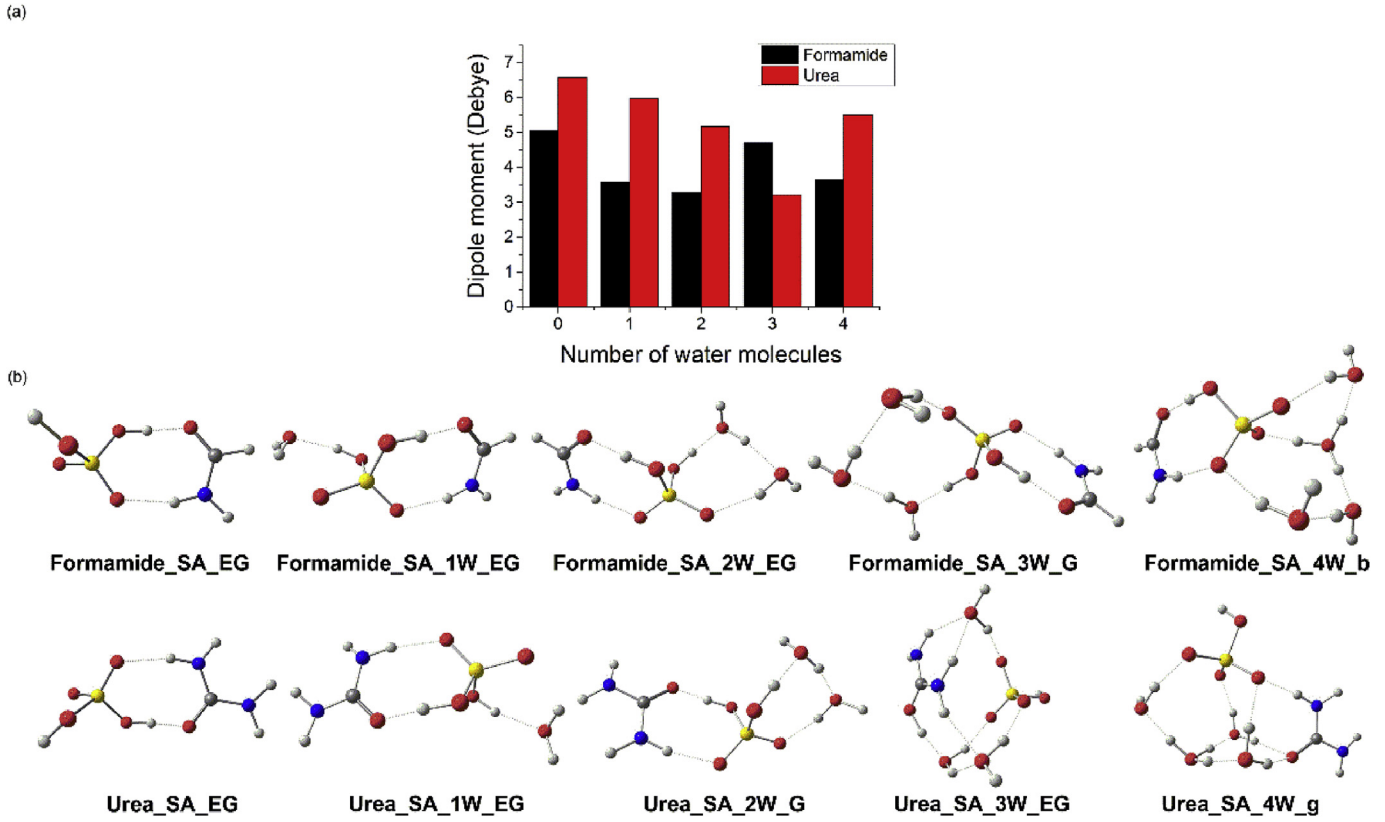

Fig. 5. The structures and dipole moment of (Formamide)(SA)$(W)_n$ (n = 0–4) and (Urea)(SA)$(W)_n$ (n = 0–4) clusters: (a) The dipole moment of selected isomers of (Formamide)(SA)$(W)_n$ (n = 0–4) and (Urea)(SA)$(W)_n$ (n = 0–4) clusters. (b) The corresponding structures of selected isomers calculated at the M06-2X/6-311++G(3df,3pd) level of theory (oxygen in red, hydrogen in white, sulfur in yellow, carbon in gray and nitrogen in blue). (For interpretation of the references to colour in this figure legend, the reader is referred to the Web version of this article.)

moment of **Formamide_SA_3W_G** and **Urea_SA_4W_EG**, however, formamide hydrate clusters with more than 2 water molecules and urea with more than 3 water molecules are almost non-existent at various RH (298.15 K), as indicated by the hydrate distributions in Fig. 3. The dipole moment of **Formamide_SA_EG** is comparable to the reported highest ones of mono-, di-, and trihydrates of the sulfuric acid (3.8, 5.03 and 4.16 Debye, respectively) (Nadykto and Yu, 2008) while that of **Urea_SA_EG** is higher. This indicates that (Amide)(SA) clusters have similar or even higher ability than hydrated SA clusters to participate in ion-induced nucleation. As can be seen from Fig. 5b, amide clusters with high dipole moment tend to be linear structure. The dipole moment decreases when structure changes to spherical, as in the case of **Urea_SA_3W_EG**. Overall, the dipole moment of urea clusters is higher than that of formamide clusters except for **Urea_SA_3W_EG**.

4. Conclusions

In this work, quantum chemical calculations have been performed to investigate the interactions of urea and formamide with sulfuric acid (SA) and up to four water (W) molecules at the M06-2X/6-311++G(3df,3pd) level of theory. The geometries and properties of (Formamide)(SA)$(W)_n$ ($n = 0–4$) and (Urea)(SA)$(W)_n$ ($n = 0–4$) clusters were investigated. Results show that amide and SA tend to form cyclic structure through C═O and NH_2 groups and the C═O group plays more important role in the interaction between amides and SA. The differences of cluster structures are partly due to the presence of additional amine group in urea providing more interaction sites. Proton transfer to C═O group would not occur in formamide clusters, indicating that the proton transfer depends on the structure of amide compounds. Meanwhile, proton transfer in amide clusters only occurs in highly hydrated clusters and the proton transfer to water molecule in highly hydrated urea clusters become dominant only at low temperatures. From thermodynamic analysis, the intermolecular interaction of (Formamide)(SA) is weaker than that of (Urea)(SA) and SA dimer, indicating the significant effect of amine group on the stabilizing effect of amides toward SA. However, the high concentration of formamide may be able to compensate the relatively unfavorable interaction between formamide and SA, thus enabling formamide to participate in initial steps of NPF. Moreover, water affinity is characteristic for formamide clusters which is demonstrated by hydrate distributions that the percentage of hydrated formamide clusters become dominant in higher RH. The Rayleigh light scattering intensities of amide clusters are comparable to that of amine and oxalic acid clusters reported previously. Besides, the Rayleigh light scattering intensities of urea clusters are higher than formamide clusters which may due to the enhancing effect of amine group. Moreover, unhydrated (Amide)(SA) clusters, with dipole moment similar to or even higher than hydrated SA clusters, may be able to participate in ion-induced nucleation. And, the hydration may decrease the dipole moment of amide clusters thus weakening their ion-dipole interaction with ions or ionic clusters. This study may bring new insight into the role of amides in initial steps of new particle formation from molecular scale. The importance of this process for amides along with their multiphase uptake by atmospheric acidic particles should also be noticed, which needs further studies.

Acknowledgements

This work was supported by the National Key Research and Development Program of China (2016YFC0202200) and the Fundamental Research Funds for the Central Universities (DUT18GJ201, DUT18RC(3)002). The authors also thank the Network and Information Center of the Dalian University of Technology for part of computational resources.

Appendix A. Supplementary data

Supplementary data to this article can be found online at https://doi.org/10.1016/j.chemosphere.2018.09.068.

References

Almeida, J., Schobesberger, S., Kurten, A., Ortega, I.K., et al., 2013. Molecular understanding of sulphuric acid-amine particle nucleation in the atmosphere. Nature 502 (7471), 359–363.
Borduas, N., da Silva, G., Murphy, J.G., Abbatt, J.P., 2015. Experimental and theoretical understanding of the gas phase oxidation of atmospheric amides with OH radicals: kinetics, products, and mechanisms. J. Phys. Chem. 119 (19), 4298–4308.
Borduas, N., Abbatt, J.P., Murphy, J.G., So, S., da Silva, G., 2016. Gas-Phase mechanisms of the reactions of reduced organic nitrogen compounds with OH radicals. Environ. Sci. Technol. 50 (21), 11723–11734.
Bunkan, A.J., Mikoviny, T., Nielsen, C.J., Wisthaler, A., Zhu, L., 2016. Experimental and theoretical study of the OH-initiated photo-oxidation of formamide. J. Phys. Chem. 120 (8), 1222–1230.
Chen, H., Wang, M., Yao, L., Chen, J., Wang, L., 2017. Uptake of gaseous alkylamides by suspended sulfuric acid particles: formation of ammonium/aminium salts. Environ. Sci. Technol. 51 (20), 11710–11717.
Chen, J., Jiang, S., Liu, Y.-R., Huang, T., Wang, C.-Y., Miao, S.-K., Wang, Z.-Q., Zhang, Y., Huang, W., 2017. Interaction of oxalic acid with dimethylamine and its atmospheric implications. RSC Adv. 7 (11), 6374–6388.
Dimitriou, K., Kassomenos, P., 2017. Airborne heavy metals in two cities of north rhine westphalia–performing inhalation cancer risk assessment in terms of atmospheric circulation. Chemosphere 186, 78–87.
Elm, J., Bilde, M., Mikkelsen, K.V., 2012. Assessment of density functional theory in predicting structures and free energies of reaction of atmospheric pre-nucleation clusters. J. Chem. Theor. Comput. 8 (6), 2071–2077.
Elm, J., Norman, P., Bilde, M., Mikkelsen, K.V., 2014. Computational study of the Rayleigh light scattering properties of atmospheric pre-nucleation clusters. Phys. Chem. Chem. Phys. 16 (22), 10883–10890.
Elm, J., Kurten, T., Bilde, M., Mikkelsen, K.V., 2014. Molecular interaction of pinic acid with sulfuric acid: exploring the thermodynamic landscape of cluster growth. J. Phys. Chem. 118 (36), 7892–7900.
Elm, J., Myllys, N., Kurtén, T., 2016. Phosphoric acid – a potentially elusive participant in atmospheric new particle formation. Mol. Phys. 115 (17–18), 2168–2179.
Frisch, M.J., Trucks, G.W., Schlegel, H.B., Scuseria, G.E., Robb, M.A., Cheeseman, J.R., et al., 2009. Gaussian 09.
Ge, X., Wexler, A.S., Clegg, S.L., 2011. Atmospheric amines – Part I. A review. Atmos. Environ. 45 (3), 524–546.
Ge, P., Luo, G., Luo, Y., Huang, W., Xie, H., Chen, J., Qu, J., 2018. Molecular understanding of the interaction of amino acids with sulfuric acid in the presence of water and the atmospheric implication. Chemosphere 210, 215–223.
Glasoe, W.A., Volz, K., Panta, B., Freshour, N., Bachman, R., Hanson, D.R., McMurry, P.H., Jen, C., 2015. Sulfuric acid nucleation: an experimental study of the effect of seven bases. J. Geophys. Res. Atmos. 120 (5), 1933–1950.
Hanson, D.R., Eisele, F., 2000. Diffusion of H_2SO_4 in humidified Nitrogen: hydrated H_2SO_4. J. Phys. Chem. 104 (8), 1715–1719.
Haywood, J., Boucher, O., 2000. Estimates of the direct and indirect radiative forcing due to tropospheric aerosols: a review. Rev. Geophys. 38 (4), 513–543.
Kuang, C., McMurry, P.H., McCormick, A.V., Eisele, F.L., 2008. Dependence of nucleation rates on sulfuric acid vapor concentration in diverse atmospheric locations. J. Geophys. Res. 113, D10209.
Kumar, M., Trabelsi, T., Francisco, J.S., 2018. Can urea Be a seed for aerosol particle formation in air? J. Phys. Chem. 122 (12), 3261–3269.
Lin, X.-X., Liu, Y.-R., Huang, T., Xu, K.-M., Zhang, Y., Jiang, S., Gai, Y.-B., Zhang, W.-J., Huang, W., 2014. Theoretical studies of the hydration reactions of stabilized criegee intermediates from the ozonolysis of β-pinene. RSC Adv. 4 (54), 28490–28498.
Luo, Y., Maeda, S., Ohno, K., 2007. Quantum chemistry study of $H^+(H_2O)_8$: a global search for its isomers by the scaled hypersphere search method, and its thermal behavior. J. Phys. Chem. 111 (42), 10732–10737.
Lv, S.S., Miao, S.K., Ma, Y., Zhang, M.M., Wen, Y., Wang, C.Y., Zhu, Y.P., Huang, W., 2015. Properties and atmospheric implication of methylamine-sulfuric acid-water clusters. J. Phys. Chem. 119 (32), 8657–8666.
Maeda, S., Ohno, K., 2005. Global mapping of equilibrium and transition structures on potential energy surfaces by the scaled hypersphere search Method: applications to ab initio surfaces of formaldehyde and propyne molecules. J. Phys. Chem. 109 (25), 5742–5753.
Maeda, S., Ohno, K., 2007. Structures of water octamers $(H_2O)_8$: exploration on ab initio potential energy surfaces by the scaled hypersphere search method. J. Phys. Chem. 111 (20), 4527–4534.
Maeda, S., Ohno, K., 2008. Microsolvation of hydrogen Sulfide: exploration of $H_2S{\cdot}(H_2O)_n$ and $SH^-{\cdot}H_3O^+{\cdot}(H_2O)_{n-1}$ ($n = 5–7$) cluster structures on ab initio

potential energy surfaces by the scaled hypersphere search method. J. Phys. Chem. 112 (13), 2962–2968.
Metzger, A., Verheggen, B., Dommen, J., Duplissy, J., Prevot, A.S., Weingartner, E., Riipinen, I., Kulmala, M., Spracklen, D.V., Carslaw, K.S., Baltensperger, U., 2010. Evidence for the role of organics in aerosol particle formation under atmospheric conditions. Proc. Natl. Acad. Sci. U. S. A. 107 (15), 6646–6651.
Miao, S.-K., Jiang, S., Chen, J., Ma, Y., Zhu, Y.-P., Wen, Y., Zhang, M.-M., Huang, W., 2015. Hydration of a sulfuric acid–oxalic acid complex: acid dissociation and its atmospheric implication. RSC Adv. 5 (60), 48638–48646.
Nadykto, A.B., 2003. Uptake of neutral polar vapor molecules by charged clusters/particles: enhancement due to dipole-charge interaction. J. Geophys. Res. 108, D23.
Nadykto, A.B., Yu, F., 2007. Strong hydrogen bonding between atmospheric nucleation precursors and common organics. Chem. Phys. Lett. 435 (1–3), 14–18.
Nadykto, A.B., Yu, F., 2008. Anomalously large difference in dipole moment of isomers with nearly identical thermodynamic stability. J. Phys. Chem. 112 (31), 7222–7226.
Nadykto, A.B., Yu, F., Herb, J., 2009. Theoretical analysis of the gas-phase hydration of common atmospheric pre-nucleation $(HSO_4^-)(H_2O)_n$ and $(H_3O^+)(H_2SO_4)(H_2O)_n$ cluster ions. Chem. Phys. 360 (1–3), 67–73.
Nielsen, C.J., D'Anna, B., Dye, C., Graus, M., Karl, M., King, S., Maguto, M.M., Müller, M., Schmidbauer, N., Stenstrøm, Y., Wisthaler, A., Pedersen, S., 2011. Atmospheric chemistry of 2-aminoethanol (MEA). Energy Proced. 4, 2245–2252.
Nielsen, C.J., Herrmann, H., Weller, C., 2012. Atmospheric chemistry and environmental impact of the use of amines in carbon capture and storage (CCS). Chem. Soc. Rev. 41 (19), 6684–6704.
Noppel, M., Vehkamäki, H., Kulmala, M., 2002. An improved model for hydrate formation in sulfuric acid–water nucleation. J. Chem. Phys. 116 (1), 218–228.
Ohno, K., Maeda, S., 2004. A scaled hypersphere search method for the topography of reaction pathways on the potential energy surface. Chem. Phys. Lett. 384 (4–6), 277–282.
Ohno, K., Maeda, S., 2006. Global reaction Route mapping on potential energy surfaces of formaldehyde, formic acid, and their metal-substituted analogues. J. Phys. Chem. 110 (28), 8933–8941.
Olenius, T., Kupiainen-Maatta, O., Ortega, I.K., Kurten, T., Vehkamaki, H., 2013. Free energy barrier in the growth of sulfuric acid-ammonia and sulfuric acid-dimethylamine clusters. J. Chem. Phys. 139 (8), 084312.
Omori, K., Nakayama, H., Ishii, K., 2014. Diversity of the dimer structures of toluene: exploration by the GRRM method. Chem. Lett. 43 (11), 1803–1805.
Ortega, I.K., Kupiainen, O., Kurtén, T., Olenius, T., Wilkman, O., McGrath, M.J., Loukonen, V., Vehkamäki, H., 2012. From quantum chemical formation free energies to evaporation rates. Atmos. Chem. Phys. 12 (1), 225–235.
Partanen, L., Vehkamaki, H., Hansen, K., Elm, J., Henschel, H., Kurten, T., Halonen, R., Zapadinsky, E., 2016. Effect of conformers on free energies of atmospheric complexes. J. Phys. Chem. 120 (43), 8613–8624.
Peng, X.-Q., Liu, Y.-R., Huang, T., Jiang, S., Huang, W., 2015. Interaction of gas phase oxalic acid with ammonia and its atmospheric implications. Phys. Chem. Chem. Phys. 17 (14), 9552–9563.
Peng, X.Q., Liu, Y.R., Huang, T., Jiang, S., Huang, W., 2015. Interaction of gas phase oxalic acid with ammonia and its atmospheric implications. Phys. Chem. Chem. Phys. 17 (14), 9552–9563.
Peng, X.-Q., Huang, T., Miao, S.-K., Chen, J., Wen, H., Feng, Y.-J., Hong, Y., Wang, C.-Y., Huang, W., 2016. Hydration of oxalic acid–ammonia complex: atmospheric implication and Rayleigh-scattering properties. RSC Adv. 6 (52), 46582–46593.
Saikia, J., Narzary, B., Roy, S., Bordoloi, M., Saikia, P., Saikia, B.K., 2016. Nanominerals, fullerene aggregates, and hazardous elements in coal and coal combustion-generated aerosols: an environmental and toxicological assessment. Chemosphere 164, 84–91.
Temelso, B., Phan, T.N., Shields, G.C., 2012. Computational study of the hydration of sulfuric acid dimers: implications for acid dissociation and aerosol formation. J. Phys. Chem. 116 (39), 9745–9758.
Temelso, B., Morrell, T.E., Shields, R.M., Allodi, M.A., Wood, E.K., Kirschner, K.N., Castonguay, T.C., Archer, K.A., Shields, G.C., 2012. Quantum mechanical study of sulfuric acid hydration: atmospheric implications. J. Phys. Chem. 116 (9), 2209–2224.
Von Schneidemesser, E., Monks, P.S., Allan, J.D., Bruhwiler, L., Forster, P., Fowler, D., Lauer, A., Morgan, W.T., Paasonen, P., Righi, M., Sindelarova, K., Sutton, M.A., 2015. Chemistry and the linkages between air quality and climate change. Chem. Rev. 115 (10), 3856–3897.
Xie, H.B., Li, C., He, N., Wang, C., Zhang, S., Chen, J., 2014. Atmospheric chemical reactions of monoethanolamine initiated by OH radical: mechanistic and kinetic study. Environ. Sci. Technol. 48 (3), 1700–1706.
Xie, H.-B., Elm, J., Halonen, R., Myllys, N., Kurtén, T., Kulmala, M., Vehkamäki, H., 2017. Atmospheric fate of monoethanolamine: enhancing new particle formation of sulfuric acid as an important removal process. Environ. Sci. Technol. 51 (15), 8422–8431.
Xie, H.B., Ma, F., Yu, Q., He, N., Chen, J., 2017. Computational study of the reactions of chlorine radicals with atmospheric organic compounds featuring NH_x-π-bond ($x = 1, 2$) structures. J. Phys. Chem. A 121 (8), 1657–1665.
Yao, L., Wang, M.-Y., Wang, X.-K., Liu, Y.-J., Chen, H.-F., Zheng, J., Nie, W., Ding, A.-J., Geng, F.-H., Wang, D.-F., Chen, J.-M., Worsnop, D.R., Wang, L., 2016. Detection of atmospheric gaseous amines and amides by a high-resolution time-of-flight chemical ionization mass spectrometer with protonated ethanol reagent ions. Atmos. Chem. Phys. 16 (22), 14527–14543.
Zhang, R., Khalizov, A., Wang, L., Hu, M., Xu, W., 2011. Nucleation and growth of nanoparticles in the atmosphere. Chem. Rev. 112 (3), 1957–2011.
Zhao, Y., Truhlar, D.G., 2007. The M06 suite of density functionals for main group thermochemistry, thermochemical kinetics, noncovalent interactions, excited states, and transition elements: two new functionals and systematic testing of four M06-class functionals and 12 other functionals. Theor. Chem. Acc. 120 (1–3), 215–241.
Zhao, H., Jiang, X., Du, L., 2017. Contribution of methane sulfonic acid to new particle formation in the atmosphere. Chemosphere 174, 689–699.
Zhu, L., Schade, G.W., Nielsen, C.J., 2013. Real-time monitoring of emissions from monoethanolamine-based industrial scale carbon capture facilities. Environ. Sci. Technol. 47 (24), 14306–14314.